Nanoscale

Accepted Manuscript

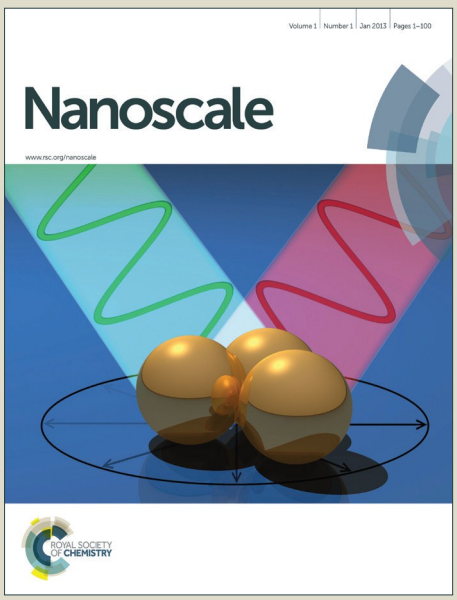

ROYAL SOCIETY OF CHEMISTRY

www.rsc.org/nanoscale

Journal Name

COMMUNICATION

Single-Molecule Imaging of DNA Polymerase I (Klenow Fragment) Activity by Atomic Force Microscopy

Received 00th January 20xx,
Accepted 00th January 20xx

DOI: 10.1039/x0xx00000x

www.rsc.org/

J. Chao,[a,c,d] P. Zhang,[b,d] Q. Wang,[a] N. Wu,[a] F. Zhang,*[b] J. Hu,[a] C. H. Fan,[a] and B. Li*[a]

We report a DNA origami-facilitated single-molecule platform that exploits atomic force microscopy to study DNA replication. We imaged several functional activities of the Klenow fragment of *E. coli* DNA polymerase I (KF) including binding, moving, and dissociation from the template DNA. Upon completion of these actions, a double-stranded DNA molecule was formed. Furthermore, the direction of KF activities was captured and then confirmed by shifting the KF binding sites on the template DNA.

Directly imaging molecular events at the nanometre scale is important for understanding complex biological processes. Atomic force microscopy (AFM) is a powerful tool for monitoring the behaviour of individual molecules in near-physiological environments at high resolution and has provided important information on DNA-protein interactions.[1] For example, the function of RNA polymerase (RNAp) and interactions between DNA and RNAp have been elucidated at the single-molecule level.[2] However, despite its similarities to RNAp in terms of structure and catalytic mechanism, characterizing the activities of DNA polymerase (DNAp) remains challenging.[3]

DNAp plays a central role in many biological processes and is an essential factor in DNA replication; the latter function can be exploited in various biotechnology applications, e.g. DNA sequencing, since it involves synthesis of a single strand of DNA from a DNA template.[4] Visualising the dynamics of DNAp activity will provide a deeper understanding of its catalytic mechanism and may also help to improve its performance in practical applications such as nanoparticle PCR.[5]

The lack of robust information on DNAp behaviour can be attributed to several issues. First, multiple components (e.g. DNA, DNAp, and dNTPs) are present during DNAp-driven DNA replication; thus, background noise partially arising from sample preparation tends to obscure object detection. This can lead to misinterpretation of data based on topographical images obtained with AFM. Second, multiple steps in the replicative process are linked (e.g. proofreading and polymerization). The forward and backward movements of DNAp can be impeded by the adsorption of DNAp as well as by DNA on a surface. Third, conformational rearrangements in both primer-template DNA and DNAp are involved.[6] Under this unique situation, the subtle effects of the interface force between DNA/DNAp and their supporting surface prevents DNA polymerization from occurring or from being detected if the force is too strong or weak, respectively. In AFM, this inherent paradox makes detection of the dynamic process more difficult.[7]

A potential solution to these problems is to combine AFM with an emerging technology known as DNA origami.[8] Programmed DNA origami has been used to study biological activities at the single-molecule level and has revealed some important DNA-protein interactions.[9] We have shown that a single-molecule recognition reaction can be captured and tuned on a DNA origami nanostructure.[10] In the present study, we used AFM to investigate the interaction between DNAp and the template during replication using DNA origami as a platform.

In our experimental set-up, the template DNA was introduced into the middle of an equilateral triangular DNA origami. The two ends of the template were connected to the midpoint of one side of the triangle and the opposing vertex, respectively (Fig. 1). The approximate length of the 74-nt template, i.e. >45.0 nm (if each base is 6.3 Å[11]), across the length of the DNA origami (<45.0 nm, the theoretical distance of the height) could offer a means of detecting DNAp activity during replication by time-lapse AFM. Polymerization on a surface

[a] Division of Physical Biology & Bioimaging Center, Shanghai Synchrotron Radiation Facility, CAS Key Laboratory of Interfacial Physics and Technology, Shanghai Institute of Applied Physics, Chinese Academy of Sciences, Shanghai 201800, China. Email:libin@sinap.ac.cn; fengzhang1978@hotmail.com

[b] Agricultural Nanocenter, School of Life Science, Inner Mongolia Agricultural University, 306 Zhaowuda Road, Hohhot 010018, China

[c] Key Laboratory for Organic Electronics and Information Displays & Institute of Advanced Materials, Jiangsu National Synergetic Innovation Center for Advanced Materials, Nanjing University of Posts & Telecommunications, 9 Wenyuan Road,

was facilitated by a fully functional polymerase Klenow fragment (KF), which is significantly smaller than DNAp I.[12]

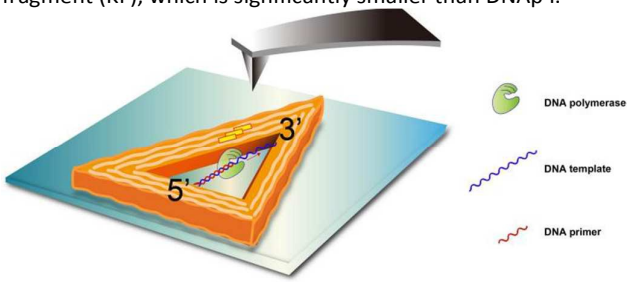

Figure 1. Schematic illustration of the experimental set-up for examining DNA polymerization using AFM. The Klenow fragment (green) of DNAp I was used to replicate a single-stranded template (blue). The template DNA was located inside the triangular DNA origami (yellow) with its two ends at the base and the opposite vertex, respectively.

To form the 74-nt template DNA with its two ends attached to the DNA origami, a scaffold DNA origami nanostructure was constructed as described by Rothemund,[8a] with the exception that we selected two 'staple strands', A17 and C33, with extending sequences to produce two sticky ends (overhangs) to bind to the template DNA (Fig. S1). The self-assembly of DNA origami was conducted as previously described.[13] Briefly, the circular M13mp18 viral DNA and over 200 short oligonucleotide staple strands were mixed in TAE/Mg^{2+} buffer at a molar ratio of 1:10 and then incubated and annealed in the PCR instrument (Eppendorf Mastercycler Personal Machine) from 95 °C to 20 °C at a rate of 0.1 °C/10 s. The resulting solution was subjected to filtration (Sephacryl S-300 HR, GE Healthcare) with TAE/Mg^{2+} buffer to remove excess staple strands. Subsequently, the concentration of DNA origami was estimated by measuring the absorbance at 260 nm. Thereafter, an excess of template DNA was hybridized with DNA origami in the PCR instrument from 50 °C to 15 °C at a rate of 0.5 °C/min, and then purified using the aforementioned filtration process to remove excess template DNA. The sequence of the 74-nt template DNA with an additional 20 nt (complementary to staple strands A17 and C33, respectively) at each end was produced according to the design of oligonucleotides.[8d] (see Supporting Information for the sequences of staple strands A17 and C33 included the origami regions and extended sticky ends.)

Time-lapse AFM imaging and analysis was performed following a previously described method.[13] Briefly, a 3-μL drop of DNA origami was placed on a freshly cleaved mica surface for 5 min, and then 40 μL TAE/Mg^{2+} buffer was added. Data were collected before and after a mixture of KF and dNTPs was slowly injected into a liquid cell mounted on the 'J' scanner. The final concentrations of KF, dNTPs, and DNA origami for AFM imaging were 0.1–0.5 U/μL, 0.1–0.5 mM, and 0.5–3.0 nM, respectively. All tapping mode images were collected using a Nanoscope IIIa-Multimode AFM (Veeco-Digital Instruments, Santa Barbara, CA, USA) with a probe spring constant of ~0.35 N/m (Bruker, Germany). The scanning speed was limited to 2 Hz, and a minimal scanning force was applied. All images were flattened and analysed using NanoScope Analysis software.

To carry out a Förster resonance energy transfer experiment (FRET), we designed a Cy3/Cy5 coupling system in which each DNA origami was modified by one Cy3 molecule. The Cy3 molecule is on the vertex of triangular origami at the end of the A17 staple strand (5´-Cy3-A17), i.e. one end of template DNA at a G residue (see Supporting Information on the Cy3 labelling position on the sequence of A17). A mixture of dNTPs in which Cy5-dCTP replaced dCTP was added in the FRET experiments. Fluorescence spectra were measured on a fluorometer (Hitachi F-4500 Ultraviolet spectrophotometer, Japan).

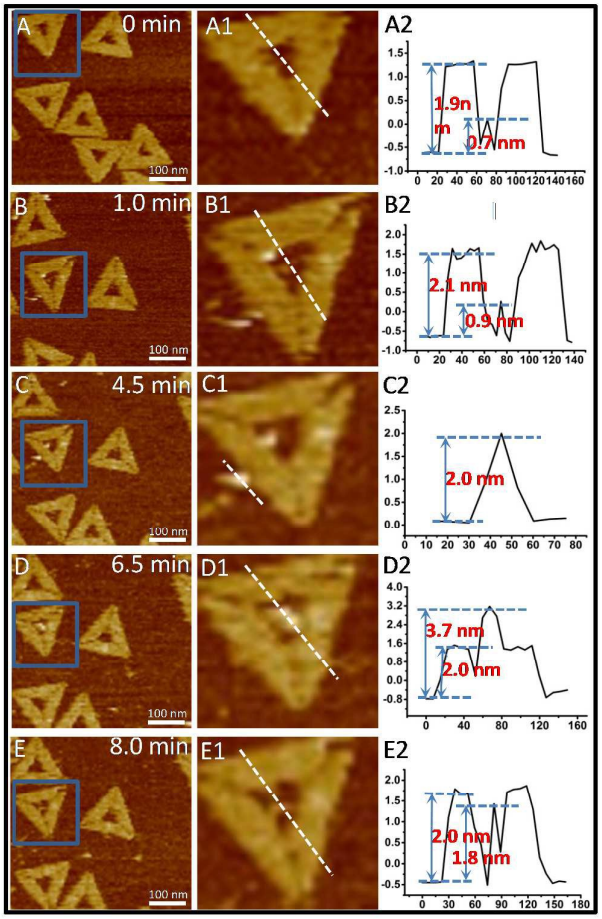

Figure 2. Representative AFM images of the stepwise movements of a single KF molecule on the DNA template during replication. (A–E) Discrete steps of a single KF molecule during polymerization, which consisted of (A–C) binding, (C and D) movement, and (E) dissociation in the presence of KF and dNTPs at ~0.0, 1.0, 4.5, 6.5, and 8.0 min, respectively. (A1,

A2, B1, B2 and E1, E2) Enlarged images of topography and height profiles of representative DNA sizes selected from the blue squares in (A), (B) and (E), respectively. An apparent increase in the height of DNA was observed following KF activities. (C1, C2 and D1, D2) Enlarged images of topography and height profiles of representative KF sizes selected from the blue squares in (C) and (D), respectively.

To clarify the features of the resulting DNA origami and associated single-stranded DNA (ssDNA) and KF, several AFM images were obtained. The results suggested that the ssDNA efficiently spans the origami; the ssDNA and dsDNA could be distinguished by height measurements (Fig. S2). Then, the DNA replication process was detected by time-lapse AFM. In Fig. 2A–E, the ssDNA with its two ends fixed on the origami was replicated by KF to yield a double-stranded DNA (dsDNA) molecule. Fig. 2A, B show the images before and immediately after adding KF. The measured lengths of the three outer and inner sides and the thickness of the triangular origami were ~120 nm, ~35 nm, and 1.9–2.1 nm, respectively, comprising the designed origami structure and the theoretical height of dsDNA. After KF was added ~4.5 min, a dot assumed to be a single KF molecule (height: ~2.0 nm) alit on a single origami (blue square in Fig. 2C). The dot appeared at the intersection of the base and height of the triangle where the terminus of the staple strand (acting as the primer) was a 3'-OH group. Over the course of the 8-min scan, the position of the dot changed from the base to the middle (Fig. 2C, D) and finally disappeared (Fig. 2E). The trajectory of the dot followed the linear track of the DNA template and was consistent with the 5'→3' direction of DNA replication (movie S1). A key finding was the apparent change in the size of the DNA following displacement of the KF; specifically, the DNA height increased from 0.9 to 1.8 nm (Fig. B2, E2), consistent with the estimated sizes of ssDNA and dsDNA, respectively.[14]

In this experiment, the DNA origami served as a platform for investigating DNA-KF interactions in a low-noise and label-free manner. In addition, its programmed geometry—i.e. the shape of the triangle here—facilitated the identification of KF movement direction on a one-dimensional DNA template. There were insufficient data to analyse the replication rate on the mica surface, which was slower than that of KF in bulk systems (~15 nt/s).[15] However, the way in which the template DNA was fixed with its two ends on the origami provided sufficient spatial freedom on the mica surface to tolerate conformational changes in the KF-DNA complex. This allowed changes in DNA and KF to be perceived by an AFM probe before and after DNA replication.

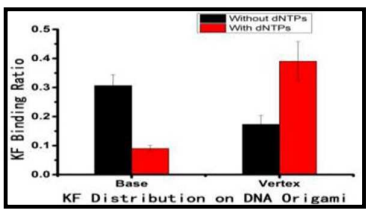

Figure 3. Histogram of KF distribution on DNA origami with and without dNTPs. In the presence of dNTPs (red), the binding ratio of the KF at the vertex of the DNA origami was higher than at the base. In the absence of dNTPs (black), the binding ratio of the KF at the base was higher than at the vertex. Error bars indicate the standard deviation of three independent experiments counting a total of 142 origami with dNTPs and 183 origami without dNTPs.

To determine whether the moving dots were functional KFs, we identified the initial binding sites of the KFs on the DNA template and the direction of movement during the reaction. For simplicity, this reaction was first carried out in vitro and then detected in a liquid cell on a freshly cleaved mica surface (Fig. S3). To discern the binding sites of single KF molecules on the template, the triangular origami was divided into two parts—i.e. the base and the vertex—at the midpoint of the height. This revealed that about 48% (with dNTPs) and 47% (without dNTPs) of the origami, respectively, exhibited binding dots. In the presence of dNTPs, 39.0% ± 6.7% of the dots were present at the vertex, and 9.0% ± 1.0% were at the base. In the absence of dNTPs, 17.3% ± 3.1% of the dots were present at the vertex, and 30.7% ± 3.8% were at the base. Although small changes were observed at other sites, the distinctive distribution of dots between the vertex and base suggests the directional movement of the KF in the presence of dNTPs. In this context, the catalytic activity of the KF on ssDNA likely reduced binding at the base and increased binding at the vertex during a given period. Taken together, these data imply that the moving object was indeed the KF molecule, and its direction of movement was the same as that observed during DNA replication (i.e. from the 5' to the 3' end). It is worth noting that dots were also detected in the three corners of the DNA origami triangles (Fig. S3 (a1)), consistent with the presence of ssDNAs in these areas; this is characteristic of the triangular design of DNA origami.[8a] More importantly, the measured heights of DNA strands were ~0.8 nm for dots at the base in the absence of dNTPs and ~1.8 nm for dots at vertex in the presence of dNTPs (Fig. S4), which further supported formation of dsDNA by a functional KF after moving along the template DNA from the base to the vertex of the DNA origami.

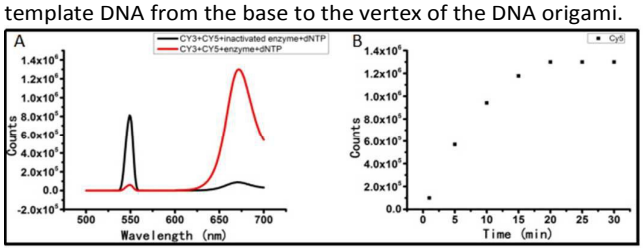

Figure 4. A Cy3-Cy5 FRET pair used for observation of DNA replication in a bulk system. (A) The FRET efficiency of Cy3-Cy5 after addition of KF as a result of DNA replication. (B) The fluorescence intensity of Cy5 as a function of reaction time in the presence of KF.

To confirm that dsDNA was produced due to replication of the template DNA of the DNA origami, we performed FRET experiments. In the absence of KF or in the presence of denatured KF, Cy3 emission was high, and Cy5 emission was low. In the presence of KF, there was a shift in the fluorescence ratio. Specifically, Cy5 fluorescence dramatically

increased, and this was accompanied by decreased Cy3 fluorescence (Fig. 4A). The ratio of Cy3/Cy5 fluorescence was reduced ~200-fold. This shift in fluorescence emission suggested a high FRET effect of donor Cy3 and receptor Cy5, consistent with DNA replication events occurring on the template DNA. To capture the reaction process, a low concentration of KF (at a final concentration of 0.01-0.05 U/μL instead of 0.1 U/μL) was used to reduce replication speed. In the presence of KF, the fluorescence intensity of Cy5 increased gradually during the first 15 min before reaching a plateau at about 20 min (Fig. 4B). The change in fluorescence intensity as a function of reaction time suggested that C-G complementary pairs accumulated over time, revealing a dynamic process of DNA replication in bulk solution. Both fluorescence experiment results exhibited an effective FRET due to DNA replication on the template DNA of DNA origami.

In summary, by combining AFM with DNA origami, we visualized the process of DNA replication through the movement of KF along an ssDNA template and the consequent generation of dsDNA. The DNA origami facilitated the fixation of ssDNA to a surface, which provided a reasonable interface environment for KF enzyme activity and afforded a well-balanced platform for studying the behaviours of single molecules in real-time. This approach is highly suited to investigation of DNA-protein interactions at the single-molecule level.

Acknowledgments

This work was supported by the National Natural Science Foundation of China (Nos. 11375253 and 11405250), the National Basic Research Program of China (973 Program 2013CB932800 and 2012CB932600), and the Chinese Academy of Sciences (KJCX2-EW-N03).

References

1 a) T. Ando, *Curr. Opin. Struct. Biol.* **2014**, *28*, 63–68. b) M. Endo, H. Sugiyama, *Accounts Chem. Res.* **2014**, *47*, 1645–1653. c) Y. Kim, B. C. Shim, S. M. Cho, J. S. Lee, J. W. Park, *J. Am. Chem. Soc.* **2014**, *136*, 13754–13760. d) D. Fotiadis, Y. Liang, S. Filipek, D. A. Saperstein, A. Engel, K. Palczewski, *Nature,* **2003**, *421*, 127–128. e) A. Raab, W. H. Han, D. Badt, S. J. Smith-Gill, S. M. Lindsay, H. Schindler, P. Hinterdorfer, *Nat. Biotechnol.* **1999**, *17*, 902–905.

2 a) M. Endo, K. Tatsumi, K. Terushima, Y. Katsuda, K. Hidaka, Y. Harada, H. Sugiyama, *Angew. Chem. Int. Ed.* **2012**, *51*, 8778–8782. b) N. H. Thomson, D. J. Billingsley, O. Chammas, N. Crampton, J. Kirkham, W. A. Bonass, *Biophys. J.* **2013**, *104*, 365a. c) N. Crampton, W. A. Bonass, J. Kirkham, C. Rivetti, N. H. Thomson, *Nucleic Acids Res.* **2006**, *34*, 5416–5425. d) H. G. Hansma, R. Golan, W. Hsieh, S. L. Daubendiek, E. T. Kool, *Struct. Biol.* **1999**, *127*, 240–247. e) C. Rivetti, M. Guthold, C. Bustamante, *J. Microsc.* **1999**, *18*, 4464–4475. f) N. H. Thomson, B. L. Smith, N. Almqvist, L. Schmitt, M. Kashlev, E. T. Kool, P. K. Hansma, *Biophys. J.* **1999**, *76*, 1024–1033. g) S.Kasas, N. H. Thomson, B. L. Smith, H. G. Hansma, X. S. Zhu, M. Guthold, C. Bustamante, E. T. Kool, M. Kashlev, P. K. Hansma, *Biochemistry* **1997**, 36, 461-468. g) Y. Suzuki, M. Shin, A. Yoshida, S. H. Yoshimura, K. Takeyasu, *FEBS Lett*. **2012**, 586, 3187–3192. i) Y. Suzuki, M. Endo, H. Sugiyama, *Methods* **2015**, 86, 4–9.

3 a) G. X. Gao, M. Orlova, M. M. Georgiadis, W. A. Hendrickson, S. P. Goff, *Proc. Natl. Acad. Sci. U.S.A.* **1997**, *94*, 407–411. b) C. M. Joyce, T. A. Steitz, *Annu. Rev. Biochem* **1994**, *63*, 777–822. c) T. A. Steitz, S. J. Smerdon, J. Jager, C. M. Joyce, *Science* **1994**, *266*, 2022–2025.

4 a) A. Berdis, *J. Chem. Rev.* **2009**, 109, 2862–2879. b) C. A. Brautigam, T. A. Steitz, *Curr. Opin. Struc. Biol.* **1998**, *8*, 54–63.

5 a) M. Yuce, H. Kurt, V. R. S. S. Mokkapati, H. Budak, *RSC Adv.* **2014**, *4*, 36800–36814. b) S. Mandal, M. Hossain, T. Muruganandan, G. S. Kumar, K. Chaudhuri, *RSC Adv.* **2013**, *3*, 20793–20799. c) P. Chen, D. Pan, C. H. Fan, J. H. Chen, K. Huang, D. F. Wang, H. L. Zhang, Y. Li, G. Y. Feng, P. J. Liang, L. He, Y. Y. Shi, *Nat. Nanotech.* **2011**, *6*, 639–644. d) L. J. Mi, Y. Q. Wen, D. Pan, Y. H. Wang, C. H. Fan, J. Hu, *Small* **2009**, 5, 2597–2600. e) H. K. Li, J. H. Huang, J. Lv, H. J. An, X. D. Zhang, Z. Z. Zhang, C. H. Fan, J. Hu, *Angew. Chem. Int. Ed.* 2005, 44, 5100–5103.

6 a) Y. Santoso, C. M. Joyce, O. Potapova, L. Le Reste, J. Hohlbein, J. P. Torella, N. D. F. Grindley, A. N. Kapanidis, *Proc. Natl. Acad. Sci. U.S.A.* **2010**, *107*, 715–720. b) K. Datta, N. P. Johnson, P. H. von Hippel, *Proc. Natl. Acad. Sci. U.S.A.* **2010**, *107*, 17980–17985.

7 a) G. R. Abel, E. A. Josephs, N. Luong, T. Ye, *J. Am. Chem. Soc.* **2013**, *135*, 6399–6402. b) D. J. Billingsley, W. A. Bonass, N. Crampton, J. Kirkham, N. H. Thomson, *Phys. Biol.* **2012**, *9*, 021001. c) S. Kasas, N. H. Thomson, B. L. Smith, H. G. Hansma, X. S. Zhu, M. Guthold, C. Bustamante, E. T. Kool, M. Kashlev, P. K. Hansma, *Biochemistry* **1997**, *36*, 461–468.

8 a) P. W. K. Rothemund, *Nature* **2006**, *440*, 297–302. b) B. Q. Ding, Z. T. Deng, H. Yan, S. Cabrini, R. N. Zuckermann, J. Bokor, *J. Am. Chem. Soc.* **2010**, *132*, 3248–3249. C) L. Qian, Y. Wang, Z. Zhang, J. Zhao, D. Pan, Y. Zhang, Q. Liu, C. Fan, J. Hu, L. He, *Chin. Sci. Bull.* **2006**, 51, 2973-2976. d) M. Endo, Y. Katsuda, K. Hidaka, H. Sugiyama, *J. Am. Chem. Soc.* **2010**, 132, 1592-1597.

9 a) Y. Ke, S. Lindsay, Y. Chang, Y. Liu, H. Yan, *Science* **2008**, *319*, 180–183. b) N. V. Voigt, T. Torring, A. Rotaru, M. F. Jacobsen, J. B. Ravnsbaek, R. Subramani, W. Mamdouh, J. Kjems, A. Mokhir, F. Besenbacher, K. V. Gothelf, *Nat. Nanotechnol.* **2010**, *5*, 200–203. c) J. L. Fu, Y. R. Yang, A. Johnson-Buck, M. H. Liu, Y. Liu, N. G. Walter, N. W. Woodbury, H. Yan, *Nat. Nanotechnol.* **2014**, *9*, 531–536. d) Y. Suzuki, M. Endo, C. Canas, S. Ayora, J. C. Alonso, H. Sugiyama, K. Takeyasu, *Nucleic Acids Res.* **2014**, *42*, 7421–7428. e) M. Endo, H. Sugiyama, *Accounts Chem. Res.* **2014**, *47*, 1645–1653. f) Y. Suzuki, M. Endo, Y. Katsuda, K. Ou, K. Hidaka, H. Sugiyama, *J. Am. Chem. Soc.* **2014**, *136*, 211–218. g) A.H.Okholm, H. Aslan, F. Besenbacher, M Dong, J. Kjems. *Nanoscale*, **2015**, 7, 10970¬–10973.

10 a) W. Na, X. F. Zhou, D. M. Czajkowsky, M. Ye, D. D. Zeng, Y. M. Fu, C. H. Fan, J. Hu, B. Li, *Nanoscale* **2011**, *3*: 2481. b) W. Na, D. M. Czajkowsky, J. J. Zhang, J. X. Qu, M. Ye, D. D. Zeng, X. F. Zhou, J. Hu, Z. F. Shao, B. Li, C. H. Fan, *J. Am. Chem. Soc.* **2013**, *132*, 1592–1597.

11 M. Murphy, I. Rasnik, W. Cheng, T. M. Lohman, T. Ha, *Biophys. J.* **2004**, *86*, 2530–2537.

12 H. Klenow, I. Hennings, *Proc. Natl. Acad. Sci. U.S.A.* **1970**, *65*, 168–175.

13 a) N.Wu, X. F. Zhou, D. M. Czajkowsky, M. Ye, D. D. Zeng, Y. M. Fu, C. H. Fan, J. Hu, B. Li, *Nanoscale*, **2011**, 3, 2481-2484. b) N. Wu, D. M. Czajkowsky, J. J. Zhang, J. X. Qu, M. Ye, D. D. Zeng, X. F. Zhou, J. Hu, Z. F. Shao, B. Li, C. H. Fan, *J. Am. Chem. Soc.* **2013**, 135, 12172-12175.

14 a) B. Maier, D. Bensimon, V. Croquette, *Proc. Natl. Acad. Sci. U.S.A.* **2000**, *97*, 12002–12007. b) M. E. Dahlberg, S. J. Benkovic, *Biochemistry* **1991**, *30*, 4835–4843.

15 a) C. Bustamante, J. Vesenka, C. L. Tang, W. Rees, M. Guthold, R. Keller, *Biochemistry* **1992**, *31*, 22–26. b) J. J. Schwartz, S. R. Quake, *Proc. Natl. Acad. Sci. U.S.A.* **2009**, 106, 20294-20299. c) B. A. Maxwell, Z. Suo, *J. Bio. Chem.* **2013,** 288, 11590-11600.